Novel Polymer Electrolyte Composed of Poly(ethylene oxide), Lithium Triflate, and Benzimidazole

Hsien-Wei Chen,[1] HongYao Xu,[2] Chih-Feng Huang,[1] Feng-Chih Chang[1]

[1]*Institute of Applied Chemistry, National Chiao Tung University, Hsin Chu, Taiwan*
[2]*Department of Chemistry, Anhui University, Anhui, 230039, China*

Received 17 July 2002; accepted 9 June 2003

ABSTRACT: This work has demonstrated that the incorporation of benzimidazole derivatives, 2,2′-*p*-phenylene-bisindole (PPBI), enhances the ionic conductivity of a poly(ethylene oxide) (PEO)–based electrolyte by 20 times more than the plain system. Specific interactions among amino group, ethyl oxide, and lithium cation were investigated using differential scanning calorimetry (DSC), FTIR, and alternating current impedance. The DSC characterization confirms that the initial addition of PPBI is able to enhance the PEO crystallinity attributed to the interaction between the negative charge from the amino group and the lithium cation. Three types of complexes are present: complex I is present in the PEO phase, complex II resides at interphase, and complex III is located within the PPBI domain. Complex II plays the key role in stabilizing these two microstructure phases. FTIR spectra confirm that because of the presence of PPBI one is able to dissolve lithium salts more easily than in the plain electrolyte system and thus increase the fraction of free ions. © 2003 Wiley Periodicals, Inc. J Appl Polym Sci 91: 719–725, 2004

Key words: polymeric electrolytes; ionic conductivity; poly(ethylene oxide) PEO; crystal structures; microstructure

INTRODUCTION

During the past decade, considerable effort has been devoted to the development of solid polymer electrolytes with high ionic conductivity at room temperature.[1–8] The major motivation for this interest is technological application in rechargeable and high energy density power sources. Poly(ethylene oxide) (PEO)–based polymeric electrolytes are still among the most extensively studied polymeric ionic conductors because of the beneficial structure in supporting fast ion transport.[2,9–14] However, a high crystalline phase concentration still limits the conductivity of PEO-based electrolytes. Various methods have been applied to reduce the crystallinity of PEO-based electrolytes while maintaining their high flexibility and mechanical stability over a wide temperature range. One of the most convenient approaches relies on the incorporation of an organic component possessing electron lone pairs.

Benzimidazole is an organic component with thermal stability and good electronic properties, which has attracted great interest in materials science.[15–19] The incorporation of this organocomponent is able to reduce the PEO crystallinity because the chemical structure of the aromatic group creates steric hindrance. Additionally, the amino group on the structure can supply the electrons to play as a Lewis base to complex with the lithium cation. The derivative of benzimidazole, 2,2′-*p*-phenylene-bisindole (PPBI), was previously synthesized[20–25] and, in this work, blended with PEO/$LiCF_3SO_3$ to form a novel polymer electrolyte. The complicated solid-state interaction between PEO, lithium triflate salt ($LiCF_3SO_3$, LiTf), and PPBI was investigated by differential scanning calorimetry (DSC), FTIR, and alternating current (ac) impedance. Three different types of complexes were used to interpret the interaction between ethyl oxide, lithium cation, and amino group. The purpose of this work was to emphasize the extraordinary effect occurring when benzimidazole is added to the PEO/LiTf blend system.

Correspondence to: F.-C. Chang (changfc@cc.nctu.edu.tw).

Journal of Applied Polymer Science, Vol. 91, 719–725 (2004)

EXPERIMENTAL

Materials

Sample preparation

Poly(ethylene oxide) (PEO) with weight-average molecular weight of 200,000 was purchased from Aldrich (Milwaukee, WI). The lithium triflate ($LiCF_3SO_3$, LiTf), also purchased from Aldrich, was dried in a vacuum oven at 80°C for 24 h, and then stored in a desiccator before use. Acetonitrile was refluxed at a suitable temperature under nitrogen atmosphere before use. Terephthalic acid (1,4-benzenedicarbonic acid), *o*-benzenediamine, and polyphophoric acid (Aldrich) were used for synthesis of PPBI.

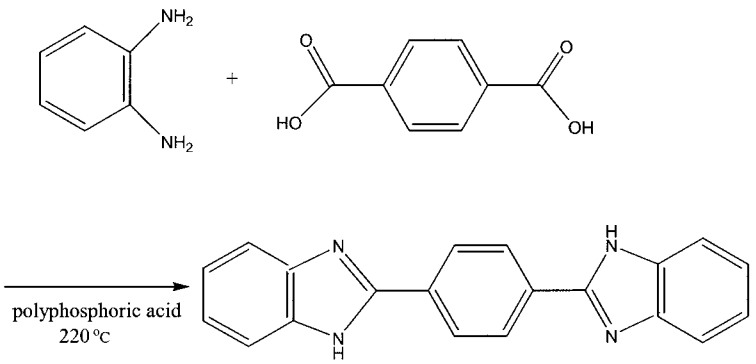

Scheme 1 Synthesis of 2,2′-*p*-phenylene-bisindole (PPBI).

Synthesis of PPBI

Terephthalic acid (2 g), *o*-benzenediamine (2.26 g), and polyphosphoric acid (20 g) were heated at 200°C under nitrogen for 3 h with constant stirring in a 200-mL beaker (**Scheme 1**). The reactant mixture was poured into 300 g of ice-distilled water with stirring and neutralized slowly by 10 wt % sodium bicarbonate ($NaHCO_3$) solution. Afterward, the precipitate was washed with water and decolorized with activated charcoal in *N*,*N*-dimethylformamide (DMF). The DMF solution was concentrated and recrystallized in a cooled environment (yield 90%).

Preparation of solid polymer electrolyte (SPE)

Desired amounts of PEO (Table I), vacuum-dried LiTf salt, and PPBI in dry acetonitrile were mixed to form PEO/PPBI/LiTf blends of varying compositions. After continuous stirring for 24 h at 80°C, these solutions were maintained at 50°C for an additional 24 h to facilitate initial solvent removal. Further drying was carried out under vacuum at 70°C for 3 days. To prevent contact with air and moisture, all compositions were stored in a dry box filled with nitrogen. All samples were equilibrated at ambient temperature for at least 1 month in a dry box before undertaking any further experiments.

Methods

Conductivity measurements

Ionic conductivity measurements with ac were conducted on an Autolab (designed by Eco Chemie) within the frequency range from 10 MHz to 10 Hz. The composite film was sandwiched between stainless steel blocking electrodes (1 cm diameter). The specimen thickness varied from 0.8 to 1.2 mm, and the impedance response was gauged at 30°C.

TABLE I
Desired Amounts for PEO/PPBI and $(PEO)_8$LiTf (wt %)

	Composition of PEO/PPBI and $(PEO)_8$/LiTf (wt %)							
Component	a	b	c	d	e	f	g	h
PEO, $(PEO)_8$LiTf	100	99	97	94	91	87	77	71
PPB1	0	1	3	6	9	13	23	29

Differential scanning calorimetry (DSC)

Thermal analysis was carried out on a DSC instrument from DuPont (DSC-9000; DuPont, Boston, MA) at a scan rate of 10°C/min ranging from −100 to 200°C. Approximately 5–10 mg of each sample was weighed and sealed in an aluminum pan for DSC analysis. The sample was quickly cooled to −100°C from the melt state (180°C) for the first scan and then scanned between −100 to 200°C at 10°C/min.

The PEO crystallinity of the electrolyte film was calculated as a ratio of the heat enthalpy of the crystalline PEO phase to the heat enthalpy of the pure crystalline PEO (165.5 J g^{-1}).[9,26,27]

Infrared spectroscopy

The conventional NaCl disk method was employed to measure infrared spectra of composite films. All polymer films were prepared under N_2 atmosphere. The acetonitrile solution was cast onto a NaCl disk from which the solvent was removed under vacuum at 70°C for 48 h. All infrared spectra were obtained at a resolution of 1 cm^{-1} on a Nicolet Avatar 320 FTIR spectrometer (Nicolet Analytical Instruments, Madison, WI) at 120°C.

RESULTS AND DISCUSSION

DSC studies

From previous studies,[9,29–31] PEO was found to form a complex with a lithium salt following the Lewis base–acid type interaction between the polyether matrix and the lithium cation. This strong Lewis base–acid interaction would format the transient crosslinks between the salt and the polyether phase resulting in

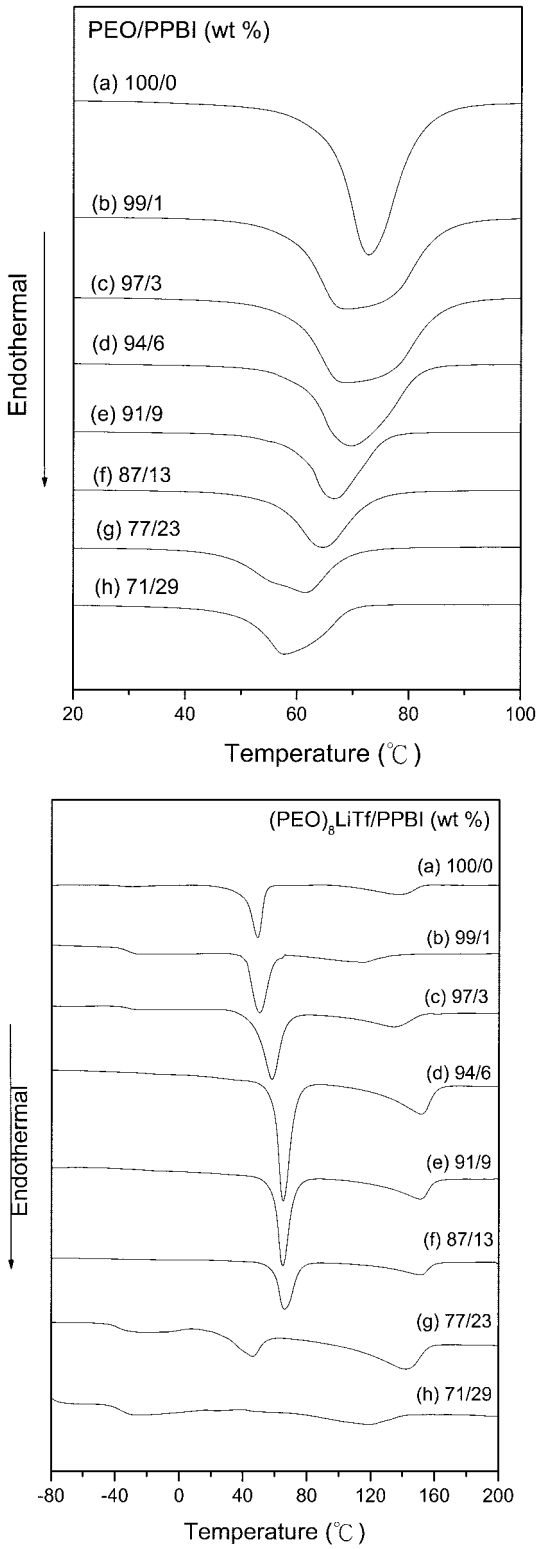

Figure 1 DSC traces obtained for different PEO-based electrolyte systems: (a) $(PEO)_8LiTf$; (b) $(PEO)_8LiTf/PPBI$.

lower crystallinity. In general, DSC analysis is one of the most convenient methods to characterize the thermal properties of a polyether chain. Figure 1 presents the conventional second-run DSC thermograms of PEO/PPBI binary blends [Fig. 1(a)] and PEO/PPBI/LiTf ternary blends [Fig. 1(b)] containing a constant content of LiTf [$EO/Li^+ = 8$, $(PEO)_8LiTf$]. As shown in Figure 1(a), the endothermic first-order transition at about 70°C can be observed, corresponding to the melting of the crystalline PEO phase. When PPBI is added, the melting peak seems composed of two distinct shoulders. This means PEO/PPBI itself may form two phases in the absence of the Li-triflate and the two phases are sufficient to create ordered structures giving a distinct melting point. However, this endothermic peak decreases progressively with the increase of the PPBI concentration and shifts toward lower temperature. The change of the PEO thermal properties is thought to be attributed to the incorporation of the PPBI, which interferes with the PEO chain arrangement and retards the PEO crystallinity. However, considerable differences can be observed when a specific amount of LiTf is added (mole ratio, $EO/Li^+ = 8$) [Fig. 1(b)]. Similar curves have been obtained for other electrolyte systems.[9,26,27] Two endothermic first-order transitions can be observed. The lower endothermic peak at 50–70°C can be attributed to the melting of the crystalline PEO phase. Additionally, a second minor endothermic peak appears at 140–150°C when the lithium salt is added. This minor endotherm is attributed to the melting of the crystalline complex phase formed between PEO and LiTf.[9,26,27] The PEO crystallinity [X_c (%)] in the $(PEO)_8LiTf/PPBI$ system is altered with the addition of PPBI. The PEO crystallinity initially increases with increasing PPBI content, reaches a maximum value at 6% PPBI, and decreases as the PPBI content is further increased. However, the change of the glass-transition temperature in the $(PEO)_8LiTf/PPBI$ system cannot be observed in DSC analyses. All the data obtained from the DSC thermograms are summarized in the Table II.

To clarify the phenomenon of increasing PEO crystallinity with the presence of a small amount of PPBI, Figure 2 shows plots of X_c (%) against PPBI content (wt %) for these two different systems. X_c (%) was calculated as a ratio of the heat enthalpy of the crystalline PEO phase to the heat enthalpy of the pure crystalline PEO (165.5 J g^{-1}) and PEO fraction in each composition. As can be seen, the X_c (%) of the undoped PEO system decreases gradually with increasing PPBI content and this phenomenon can be attributed to steric hindrance caused by the large surface area of the aromatic group in the PPBI. When the lithium salt is added, the PEO crystallinity increases initially with the increase of the PPBI content and approaches maximum crystallinity at 6% PPBI concentrations. Subsequently, the crystallinity decreases gradually with further increase in PPBI content. This observed trend in PEO crystallinity can be interpreted as a result of the complicated Lewis acid–base type

TABLE II
DSC Data for PEO-Based Polymer Electrolytes: PEO/PPBI and $(PEO)_8$ LiTf/PPBI Polymeric Electrolytes

	PEO/PPBI			
Weight percentage	T_g (°C)	T_m (°C)	ΔH_m (J g^{-1})	X_c (%)
0	—	72.8	165.5	100.0
1	−49.0	68.4	163.5	98.8
3	−43.3	68.2	157.1	94.9
6	−47.8	69.2	118.9	71.8
9	−51.1	66.3	98.8	59.7
13	−53.3	64.6	89.2	53.9
23	−52.6	61.3	75.6	45.7
29	−48.3	57.5	79.3	47.9

	$(PEO)_8$LiTf/PPB1				
Weight percentage	T_g (°C)	T_m (°C)	ΔH_m (J g^{-1})	X_c (%)	T_{mc} (°C)
0	−38	54.2	30.5	18.4	120
1	−37	46.1	39.0	23.6	111
3	−32	57.6	54.8	33.4	135
6	−36	64.6	66.0	41.1	151
9	−43	66.1	49.4	31.6	151
13	−39	46.0	17.5	11.5	143
23	−39	46.3	4.5	3.1	117
29	−35	13.7	0.8	0.6	121

interactions among polyether matrix, amino group, lithium cation, and corresponding anion.

Three types of complexes can be assigned, which are depicted in Figure 3. Complex I is present in the pure PEO phase and complex III is located within the PPBI phase. Complex II, located at the interphase, plays a key role in stabilizing these two microstructure phases. For samples of the $(PEO)_8$LiTf/PPBI system, X_c (%) increases initially up to a specific PPBI concentration and then decreases. Without containing PPBI, the $(PEO)_8$LiTf system forms only complex I. A portion of complex I tends to convert into complex II and complex III because of the strong interaction existing between Li^+ cations and amino groups of PPBI. Shifting from complex I into complex II and complex III, a portion of the original lithium cations have been drawn into the PPBI region to induce higher PEO chain flexibility and thus higher crystallinity. In this aspect, the presence of PPBI causes higher PEO crystallinity attributed to greater PEO chain flexibility. However, higher PPBI content results in forming more complex II and complex III, which can act as crystallization retarders (especially complex II) because of steric hindrance, thus leading to lower PEO crystallinity. In this system, two adverse and competitive effects occur, one of which is favorable and the other unfavorable, for the PEO crystallization.

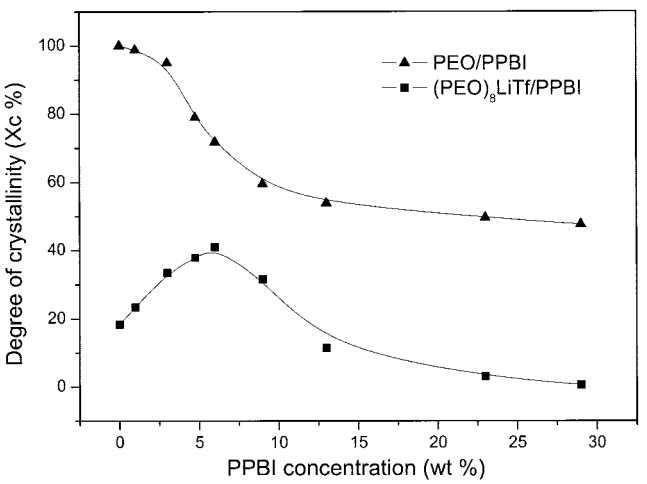

Figure 2 Degree of crystallinity [X_c (%)] versus PPBI concentration (wt %) for different PEO-based electrolytes system: (▲) PEO/PPBI; (■) $(PEO)_8$LiTf/PPBI.

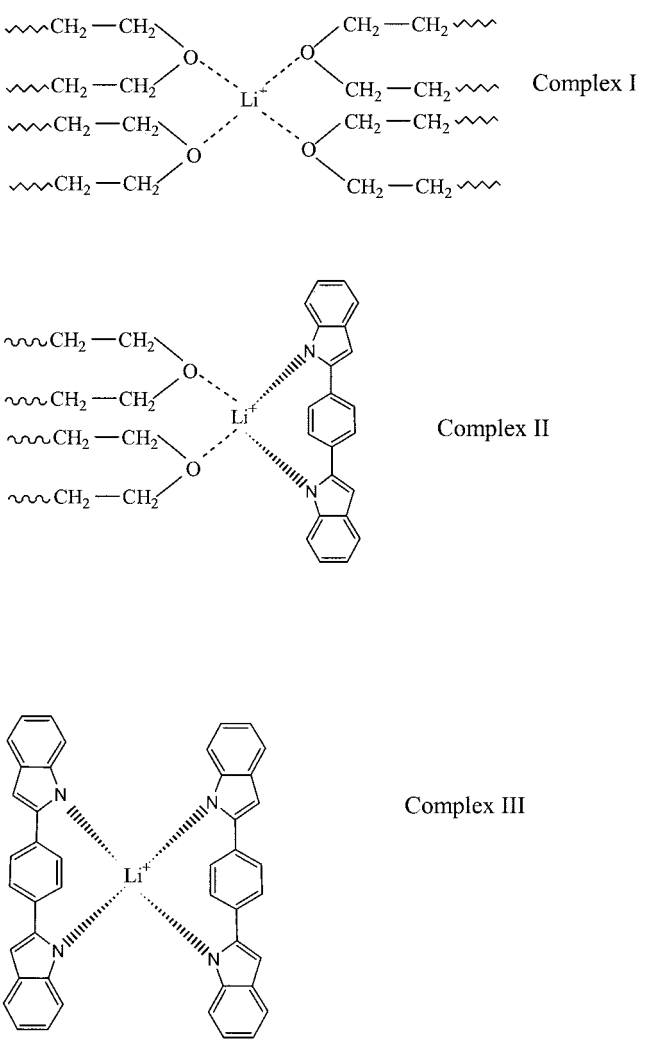

Figure 3 Schematic structure of the complex formed by Li^+ cation with (a) polyether chains (Complex I), (b) polyether and PPBI (Complex II), (c) PPBI (Complex III).

Infrared spectra

FTIR spectroscopy is a powerful tool for probing microscopic details in electrolytic systems; in particular, the characteristic $\nu_s(SO_3)$ internal mode of the $CF_3SO_3^-$ anion is sensitive in changing the local anionic environment.[28–30] According to previous studies,[28–32] the component observed at about 1031 cm^{-1} was assigned as the "free" anion, which does not interact directly with the lithium cation. Components at about 1042 and 1050–1054 cm^{-1} were attributed to contact ion pairs and $Li_2CF_3SO_3^+$ triple ions (or ionic aggregates), respectively. Figure 4 presents typical infrared spectra in the $\nu_s(SO_3)$ spectral region from 1070 to 1010 cm^{-1} for $(PEO)_8$LiTf/PPBI with various PPBI concentrations at 27°C. The shoulder of the "free" anion (~ 1031 cm^{-1}) increases gradually with increasing PPBI content and eventually attains maximum intensity when the PPBI content is 13 wt %. When the PPBI content is further increased, above 13 wt %, the intensity of the shoulder decreases gradually and approaches its original value. Meanwhile, the slight chemical shift of the "ion pair," located at 1043 cm^{-1}, is also observed with the addition of the PPBI. The band of the "ion pair" (1043 cm^{-1}) shifts to lower wavenumber when a small quantity of PPBI is added. The change of the intensity of the "free" anions (~ 1031 cm^{-1}) and the chemical shift of the "ion pairs" (~ 1043 cm^{-1}) indicate that the electrons surrounding the lithium cation have been deprived by the incorporation of PPBI. In other words, the attractive force between the lithium cation (Li^+) and anion ($CF_3SO_3^-$) is reduced by the presence of the amino group of PPBI.

Fractions of the "free" anions, shown in Figure 4, were measured by decomposing the $\nu_s(SO_3)$ band into three Gaussian peaks, respectively. In Figure 5, the fraction of "free" anions is plotted against PPBI concentration (wt %). The fraction of the "free" anion increases initially with the increase of the PPBI content and approaches a maximum at 13 wt %. Subsequently, the fraction of the "free" anion decreases gradually with further increase of the PPBI content. This observed trend in the fraction of the "free" anion is also consistent with its thermal behavior, which can be attributed to numerous Lewis acid–base type interactions among polyether matrix, amino group, lithium cation, and corresponding anion. The negative charges in the amino groups play a similar role as the polar group in PEO, to dissolve the lithium salt and affect the environment surrounding the anion. It can be concluded that the composition of $(PEO)_8$LiTf with 13 wt % PPBI creates the most suitable environment for ionic transference and produces the maximum "free" anion fraction.

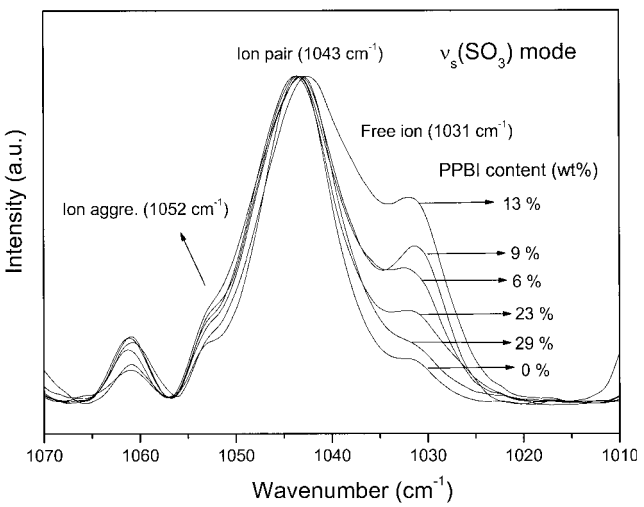

Figure 4 Infrared spectra of $\nu_s(SO_3)$ internal modes for $(PEO)_8$LiTf/PPBI electrolytes containing various PPBI concentrations.

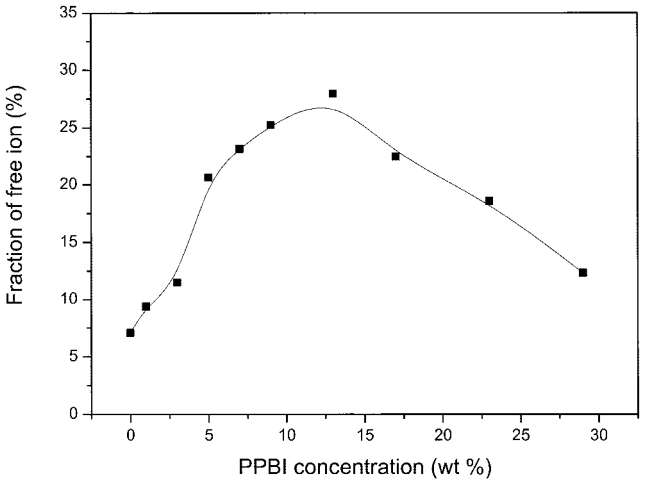

Figure 5 Fraction of "free" anions versus PPBI concentration for $(PEO)_8$LiTf/PPBI electrolytes at 27°C.

Conductivity

Figure 6 plots the conductivity versus PPBI content for PEO/PPBI and $(PEO)_8$LiTf/PPBI electrolytes systems at 30°C. In the $(PEO)_8$LiTf/PPBI electrolytes system, the conductivity increases with increase of the PPBI content and attains a maximum value when the PPBI concentration is at about 13 wt %. Subsequently, the conductivity decreases drastically with further increase of the PPBI content. However, an identical trend was not found in the PEO/PPBI composition system: the ionic conductivity is relatively lower than the $(PEO)_8$LiTf/PPBI electrolytes system for the same PPBI concentration, and the conductivity values seem to be independent of the PPBI concentration. Therefore, it could be concluded that the presence of the PPBI component cannot contribute to the ionic or electronic conductivity of the system. The interactive

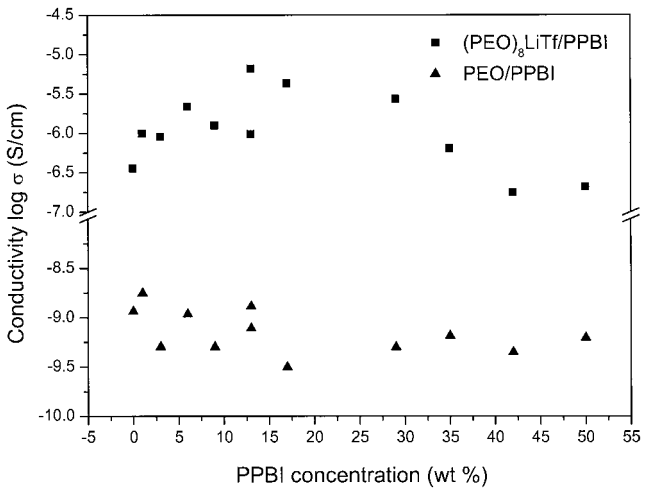

Figure 6 Ionic conductivity versus PPBI concentration (wt %) at 30°C: (▲) PEO/PPBI; (■) $(PEO)_8$LiTf/PPBI.

mechanism between the PEO/PPBI/Li can be interpreted by the trend of ionic conductivity.

The ionic conductivity (σ) of an electrolyte is defined as the product of the concentration of ionic charge carrier and its mobility according to

$$\sigma = \sum_i n_i z_i \mu_i$$

where n_i, z_i, and μ_i refer to the number of the charge carrier, ionic charge, and ionic mobility, respectively. According to the above equation, the ionic conductivity depends on the amount of charge carriers (n_i) in the system and the mobility (μ_i) of the various species. The FTIR (Fig. 5) results indicate that the addition of a specific quantity of PPBI results in the highest fraction of "free" anions and produces the highest fraction of charge carriers (higher n_i). Meanwhile, greater numbers of the relatively freer charge carrier result in higher ionic mobility (μ_i) because the strong intra-association between the lithium cation and anion have been disrupted. Therefore, enhancement of the conductivity can be expected. In the $(PEO)_8$LiTf/PPBI system, the conductivity increases nearly 20 times (8×10^{-6} S/cm) that of the $(PEO)_8$LiTf plain electrolyte (4×10^{-7} S/cm) with 13 wt % of the PPBI. This increase of the conductivity in the $(PEO)_8$LiTf/PPBI system can be attributed to the well-dispersed PPBI that tends to disrupt the intra-association of lithium salt resulting in greater numbers of the relatively freer charge carriers (n_i) and also creates higher ionic mobility (μ_i). However, excessive PPBI component in the system may interfere with the balanced attractive forces among the PEO, PPBI, and lithium cation, and result in a decrease of the observed conductivity. It can be concluded that the balanced interactions among the nitrogen group, ether group, and lithium cation and anion result in an optimum environment for ionic transport and achieve the highest ionic conductivity.

CONCLUSIONS

This study demonstrated that the addition of optimum content of PPBI increases ionic conductivity of the poly(ethyl oxide)–based electrolyte by 20 times compared to that of the plain $(PEO)_8$LiTfsystem. DSC, FTIR, and ac impedance studies indicated that strong interactions occur between the PPBI and the dopant salt LiTf within the PEO/PPBI/LiTf system. These amino groups on the PPBI interact with lithium cations to form two new types of complexes, which play the same role as the polar group in PEO. The presence of the PPBI tends to form complexes II and III at the cost of complex I of the plain electrolyte by drawing Li^+ cations away from the PEO matrix. Reduced complex I will increase the chain flexibility of the polyether and its crystallinity. However, an excess of PPBI tends to form more complex II and complex III and captures the lithium cations, thus restricting the mobility of the cation and decreasing the ionic conductivity. FTIR spectra indicate that the existence of PPBI enhances the dissolution of the lithium salt and thus increases the fraction of free anion. However, the balanced attractive forces among amino groups, ether groups, and lithium cations produce an optimum ionic conductivity.

References

1. Scrosati, B. In: Polymer Electrolyte Reviews; MacCallum, J. R.; Vincent, C. A., Eds.; Elsevier Applied Science: New York, 1989; p. 315.
2. Scrosati, B. In: Applications of Electroactive Polymers; Scrosati, B., Ed.; Chapman & Hall: New York, 1993; p. 251.
3. Armand, M. B. Solid State Ionics 1983, 9/10, 745.
4. Chao, S.; Wrighton, M. S. J Am Chem Soc 1987, 109, 2197.
5. Fenton, D. E.; Parker, J. M.; Wright, P. V. Polymer 1973, 7, 319.
6. Ratner, M. A.; Shriver, D. F. Chem Rev 1988, 88, 109.
7. Wang, L.; Yang, B.; Wang, X. L.; Tang, X. Z. J Appl Polym Sci 1999, 71, 1711.
8. Wang, X. L.; Li, H.; Tang, X. Z.; Chang, F. C. J Polym Sci Part B: Polym Phys 1999, 37, 837.
9. Wieczorek, W.; Raducha, D.; Zalewska, A.; Stevens, J. R. J Phys Chem B 1998, 102, 8725.
10. Abraham, K. M.; Jiang, Z.; Carroll, B. Chem Mater 1997, 9, 1978.
11. Yang, X. Q.; Hanson, L.; McBreen, J.; Okamoto, Y. J Power Sources 1995, 54, 198.
12. Lee, J. C.; Litt, M. H. Macromolecules 2000, 33, 1618.
13. Labreche, C.; Levesque, I.; Prud'homme, J. Macromolecules 1996, 29, 7795.
14. Mishra, R.; Rao, K. J. Solid State Ionics 1998, 106, 113.
15. Rino, L.; Hamish, M.; Dawiele, N. Tetrahedron 1995, 51, 12143.
16. Angelo, C. A.; Patricia, C.; Lucedio, G.; Pierluigi, S.; Romano, A. J Chem Soc 1991, 7, 1019.
17. Schulenberg, J. W.; Archer, S. J Org Chem 1965, 30, 1279.
18. Takahashi, S.; Kano, H. Chem Pharm Bull Jpn 1963, 11, 1375.

19. Addision, A. W.; Rao, T. N.; Wahlgren, C. G. J Heterocycl Chem 1983, 20, 1481.
20. Thompson, L. K.; Ramaswamy, B. S.; Seymour, E. A. Can J Chem 1977, 55, 878.
21. Wang, L.-Y. L.; Joullie, M. M. J Am Chem Soc 1991, 79, 5706.
22. Daydigian, J. V.; Reed, C. A. Inorg Chem 1979, 18, 2623.
23. Addison, A. W.; Burke, P. J. J Heterocycl Chem 1981, 18, 803.
24. Lee, S. I. H.; Jeoung, E. H.; Kreevoy, M. M. J Am Chem Soc 1997, 119, 2722.
25. Alberti, A.; Carloni, P.; Greci, L.; Stipa, P.; Andruzzi, R.; Marrosu, G.; Trazza, A. J Chem Soc 1991, 2, 1019.
26. Wieczorek, W.; Zalewska, A.; Raducha, D.; Florjanczyk, Z.; Stevens, J. R. Macromolecules 1996, 29, 143.
27. Wieczorek, W.; Zalewska, A.; Raducha, D.; Florjanczyk, Z.; Stevens, J. R. J Phys Chem B 1998, 10, 352.
28. Huang, W.; Frech, R.; Wheeler, R. A. J Phys Chem 1994, 98, 100.
29. Ferry, A.; Edman, L.; Forsyth, M.; MacFarlane, D. R.; Sun, J. J Appl Phys 1999, 86, 2346.
30. Ferry, A. J Phys Chem B 1997, 101, 150.
31. Huang, W.; Frech, R. Polymer 1994, 35, 235.
32. Jin, J. H.; Hong, S. U.; Won, J.; Kang, Y. S. Macromolecules 2000, 33, 4932.